Structure−Reactivity Relationships among Metallothionein Three-Metal Domains: Role of Non-Cysteine Amino Acid Residues in Lobster Metallothionein and Human Metallothionein-3

Amalia Muñoz,[†,‡] David H. Petering,*[,†] and C. Frank Shaw III*[,§]

Department of Chemistry and the UWM-NIEHS Marine and Freshwater Biomedical Science Center, University of Wisconsin—Milwaukee, Milwaukee, Wisconsin 53201-0413, and the Department of Chemistry, Eastern Kentucky University, Richmond, Kentucky 40475-3102

Received May 5, 2000

Metallothionein (MT) domains of different origins, exhibiting distinct, highly conserved cysteine positions, show differences in metal−cysteine coordination and reactivity. Lobster MT, which includes two Cd_3S_9 β domains, was chosen as a basic model to study the structure−function relationship among the clusters. The possible influence of (1) the position of the cysteine residues and (2) the steric and electrostatic effects of neighboring amino acids on the folding and stability of MT clusters have been examined with the native lobster β_C and β_N domains, each having nine cysteines and binding three M^{2+} ions, and a modified domain $\beta_{C\rightarrow N}$, in which the cysteines of the C-terminal domain are relocated so they are spaced as in the N-terminal domain. Each has been synthesized and characterized by UV, CD, ^{113}Cd NMR, and ^{1}H NMR spectroscopies. The synthetic native domains ($Cd_3\beta_C$ and $Cd_3\beta_N$) displayed spectroscopic properties, metal-binding affinities, and kinetic reactivity similar to those of the holo protein. In contrast, the modified $Cd_3\beta_{C\rightarrow N}$ domain was unusually reactive and, in the presence of Chelex, a metal-ion chelating resin, was converted to a $Cd_5(\beta_{C\rightarrow N})_2$ dimer. These differences in structure and reactivity demonstrate that the requirements for formation of a stable type-B, Cd_3S_9, β cluster are more stringent than simply the sequential positions of the cysteines along the peptide chain and include specific interactions with neighboring amino acids. Molecular mechanics calculations suggest that changes of even a single amino acid in lobster $Cd_3\beta_N$ toward lobster $Cd_3\beta_{C\rightarrow N}$ or in mammalian MT1 or MT2 toward $Cd_3\beta$-MT3 (GIF) can destabilize their structures.

Metallothionein (MT) was first discovered in horse kidney by Margoshes and Vallee in 1957.[1] It is a small molecular weight protein that lacks aromatic amino acids but is rich in cysteine residues, which confer the capacity to bind metal ions. Some of the biological functions in which MT appears to be involved are heavy-metal detoxification (Hg^{2+} and Cd^{2+}), metabolism of essential ions such as Zn^{2+} or Cu^+, detoxification of reactive oxygen species, and metabolism of electrophilic metallodrugs and alkylating agents.[2−10]

Human and mammalian MTs bind 7 Zn^{2+} or Cd^{2+} ions with 20 cysteine residues, forming two independent and dynamic clusters: type A, Cd_4S_{11}, and type B, Cd_3S_9, which constitute cores of the α (or C-terminal) and β (or N-terminal) domains of the polypeptide chain, respectively.[11−14] The folding of the protein domains depends on the thiolate−metal interactions in the two clusters; therefore, the loss of metal ions results in the disappearance of any tertiary structure.[15−17] In these clusters, cysteine sulfhydryl groups bind each Cd^{2+} with tetrahedral coordination, with some of the thiolates acting as bridging ligands between two metal ions and others serving as terminal

* To whom correspondence should be addressed.
† University of Wisconson—Milwaukee.
‡ Current address: Department of Biochemistry, University of Wisconsin—Madison, Madison, WI 53706.
§ Eastern Kentucky University.

(1) Margoshes, M.; Vallee, B. L. *J. Am. Chem. Soc.* **1957**, *79*, 4813.
(2) Shaw, C. F., III; Stillman, M. J.; Suzuki, K. T. *Metallothioneins: Synthesis, Structure and Properties of Metallothioneins, Phytochelatins and Metal−Thiolate Complexes*; Stillman, M. J., Shaw, C. F., III, Suzuki, K. T., Eds.; VCH: New York, 1991; pp 1−13.
(3) Vallee, B. L. *Methods in Enzymology 205. Metallobiochemistry. Part B. Metallothionein and Related Molecules*; Riordan, J. F., Vallee, B. L., Eds.; Academic Press Inc.: San Diego, 1991; pp 3−7.
(4) Cherian, M. G.; Chan, H. M. *Metallothionein III. Biological functions of metallothionein—A review*; Suzuki, K. T., Imura, N., Kimura, M., Eds.; Verlag Basel: Birkhäuser, Switzerland, 1993; pp 87−109.
(5) Hamer, D. *Annu. Rev. Biochem.* **1986**, *55*, 913−951.
(6) Bremner, I. *Metallothionein III: biological roles and medical implications*; Suzuki, K. T., Imura, N., Kimura, M., Eds.; Verlag Basel: Birkhäuser, Switzerland, 1993; pp 111−124.
(7) Thornally, M.; Vašák, M. *Biochim. Biophys. Acta* **1985**, *827*, 36−44.
(8) Abel, J.; De Ruiter, N. *Toxicol. Lett.* **1989**, *47*, 191−196.
(9) Endersen, L.; Bakka, A.; Rugstad, H. A. *Cancer Res.* **1983**, *43*, 2918−2926.
(10) Cagen, S. Z.; Klaassen, C. D. *Toxicol. Appl. Pharmacol.* **1979**, *51*, 107−116.
(11) Otvos, J. D.; Armitage, I. M. *Proc. Natl. Acad. Sci. U.S.A.* **1980**, *77*, 7094−7098.
(12) Robbins, A. H.; McRee, D. E.; Williamson, M.; Collett, S. A.; Xuong, N. H.; Furey, W. F.; Wang, B. C.; Stout, C. D. *J. Mol. Biol.* **1991**, *221*, 1269−1293.
(13) Robbins, A. H.; Stout, C. D. *Metallothioneins: Synthesis, Structure and Properties of Metallothioneins, Phytochelatins and Metal−Thiolate Complexes*; Stillman, M. J., Shaw, C. F., III, Suzuki, K. T., Eds.; VCH: New York, 1991; pp 31−54.
(14) Arseniev, A.; Schultze, P.; Worgotter, E.; Braun, W.; Wagner, G.; Vašák, M.; Kägi, J. H. R.; Wüthrich, K. *J. Mol. Biol.* **1988**, *201*, 637−657.
(15) Vašák, M.; Kägi, J. H. R. *Met. Ions Biol. Syst.* **1983**, *15*, 213−273.
(16) Vašák, M.; Galdes, A.; Hill, H. A. O.; Kägi, J. H. R.; Bremner, I.; Young, B. W.; *Biochemistry* **1980**, *19*, 416−425.
(17) Willner, H.; Bernhard, W. R.; Kägi, J. H. R. *Metallothioneins: Synthesis, Structure and Properties of Metallothioneins, Phytochelatins and Metal−Thiolate Complexes*; Stillman, M. J., Shaw, C. F., III, Suzuki, K. T., Eds.; VCH: New York, 1991; pp 128−143.

10.1021/ic000485s CCC: $19.00
Published on Web 11/23/2000

ligands. Previous studies demonstrated that the two domains of mammalian MTs differ in their kinetic and thermodynamic properties.[18−22] This has been related to the possibility that each domain of the protein plays different biological roles or that the presence of two different domains in the protein expands its range of reactivity with electrophilic species.[18−21]

The conserved position of the cysteine residues in MTs from different mammals suggests their importance for the formation of stable, functional clusters. Nevertheless, MTs from different phyla exhibit differences in amino acid composition, cysteine content and location, folding of the domains, and metal-ion content. Crustacean MTs are useful models for the study of MT because they exhibit limited variations in sequence and structure when compared to mammalian MTs. Lobster[23,24] and crab[25] MTs contain only 18 cysteines and 6 Cd^{2+}, which generate two type-B, Cd_3S_9 clusters each with 6 terminal and 3 bridging thiolates. Previous structural studies carried out on MT from both species by two-dimensional NMR techniques show that the Cd−cysteine coordination and, hence, the folding differ between C-terminal and N-terminal β domains (β_C and β_N, respectively) and are different from that found for the β domain in mammalian MTs.[24,25] The reactions of lobster MT with thiolate reagents such as DTNB (5,5′-dithiobis(2-nitro benzoate)) or DTP (dithiopyridine) exhibit biphasic behavior like those of mammalian MT but occur more rapidly.[26,27] Thus, both Cd−thiolate coordination and kinetic reactivity differ among these three β domains. Therefore, we propose that the reactivity is related to the detailed folding of the peptides around their clusters.

In addition to the three β domains known in crustacean and mammalian MTs, a fourth type has been identified in MT-3, the brain-specific isoform of MT also known as growth inhibitor factor (GIF). The amino acid sequence of the β domain of human GIF exhibits about 77% sequence identity with those of other mammalian MTs (MT-1 or MT-2) including the preserved location of the nine cysteine residues.[28] Nevertheless, its spectroscopic features (^{1}H NMR, CD, MCD, and electronic absorption) indicate marked structural differences with the homologous β domains of MT-1 or MT-2.[29]

In the present report, the structure−function relationships in the β domains have been studied by investigating the effect of (1) the position of the cysteine residues and (2) the charge and size of the side chain of neighboring amino acids on the Cd−SCy connectivities and, hence, on the overall folding and the reactivity of the domains. The present study includes the synthetic native lobster β_C and β_N domains and a modified $\beta_{C\rightarrow N}$ domain generated by transposition of eight amino acids, four cysteines with four other amino acids, resulting in a sequence that retains the amino acid composition and 80% of the non-cysteinyl sequence of β_C but locates the cysteine residues in the positions corresponding to those in β_N (Table 1). They have been chemically synthesized and characterized by a range of physicochemical techniques. These studies are complemented by the molecular modeling of the effect of specific amino acid substitutions on the GIF and lobster β domains.

Material and Methods

Reagents. Fmoc (9-fluroenylmethoxycarbonyl) amino acids, Fmoc−alanine−Sasrin resin, Fmoc−threonine−Sasrin resin, HOBt (1-hydroxybenzotriazole), and DCC (*N*,*N*′-dicyclohexylcarbodiimide) were purchased from Bachem. DCM (dichloromethane), NMP (*N*-methylpyrrolidone), acetonitrile, trifluoroacetic acid, ammonium sulfate, ethyl ether anhydrous, $CdCl_2$, sodium acetate, HCl, NaOH, and KCl were obtained from EM-Science. Trizma base, ninhydrin, trimethylsilyl bromine (TMSBr), *m*-cresol, and 2-mercaptoethanol were obtained from Sigma. Thioanisole was obtained from Janssen Chimica. DTNB, piperidine, and ammonium bicarbonate were obtained from Aldrich. 1,2-Ethanedithiol was obtained from Merck Shurchardt.

Peptide Synthesis, Purification, and Analysis. Automated synthesis of the β-domain sequences of lobster MT-1 was accomplished with standard Fmoc chemistry on an Applied Biosystem (abi) Peptide synthesizer 430A. The side-chain functional groups were protected as follows: *O*-*tert*-butylaspartic acid, *N*-(*tert*-butyloxycarbonyl)lysine, *O*-*tert*-butylserine, and (*S*)-Acm-cysteine.[30−32] The *N*-acetylated peptide was cleaved from all side-chain protecting groups except for Acm (acetamidomethyl) using the procedure recommended by the manufacturer. The Acm-β domains were purified by reverse-phase chromatography (Brownlee aquapore octyl 20 μm, 250 × 10 mm) in an abi HPLC, and the purity of each fraction was examined on an analytical reverse-phase HPLC column (Aquapore C_8; 300 Å, 4.6 × 30 mm). Fractions exhibiting less than 95% purity after a second chromatographic run were discarded. Electrospray mass spectrometry (ES-MS) was used to analyze and verify the identity of the Acm-β domains obtained. The experimental molecular weights were in good agreement with the theoretical values in parentheses: Acm_9-β_C, 3811 g/mol (3814); Acm_9-β_N, 3545 g/mol (3554); Acm_9-$\beta_{C\rightarrow N}$, 3815.6 g/mol (3814).

Removal of the Acm group from the cysteine sulfhydryl groups was accomplished using the mercuric acetate deprotection procedure[30−32] followed by treatment with 2-mercaptoethanol to remove Hg(II). The filtered apo peptide was purified over a Sephadex G-25 column using 20 mM acetate buffer (pH 4.0) and collected in fraction tubes containing 500 μL of 0.1 N HCl to prevent the formation of disulfide bonds. The eluted apo peptide was analyzed and characterized by UV−vis and ES-MS spectroscopies and amino acid analysis, and the absence of mercury was demonstrated by GF-AAS (graphite furnace, GBC 904 atomic absorption spectrophotometer) using 1% HNO_3 and 1% $(NH_4)_2S$. Peptide concentrations were quantitated spectrophotometrically at 570 nm using the Ruhemann's Purple method.[33] Amino acid analyses carried out in the Protein/Nucleic Acid Shared Facility of the Medical College of Wisconsin agreed well with the theoretical values in parentheses: β_C−Cys 7.1 (9), Asx 1.2 (1), Thr 3.2 (3), Ser 3.87 (4), Glx 2.3 (2), Pro 3.94 (4), Gly 1.38 (1), Ala 1.26 (1), Lys 5.27 (5); $\beta_{C\rightarrow N}$−Cys 8.1 (9), Asx 1.07 (1), Thr 3.2 (3), Ser 3.81 (4), Glx 2.29 (2), Pro 3.97 (4), Gly 1.2 (1), Ala 1.36 (1), Lys 5.3 (5); and β_N−Cys 7.4 (9), Asx 1.2 (1), Thr 2.02 (2), Ser 0.99 (1), Glx 2.3 (2), Pro 1.9 (2), Gly 4.5 (4), Ala 1.9 (2), Lys 4.35 (4), Arg 0.97 (1) (Cys determination error after performing acid oxidation averages −17%).

Mass Spectroscopy. The Acm-protected peptides, the purified apo-β peptides, and their $Cd_3\beta$ derivatives dissolved in a mixture of 50%

(18) Bernhard, W. R.; Vašák, M.; Kägi, J. H. R. *Biochemistry* **1985**, *25*, 1975−1980.
(19) Otvos, J. D.; Liu, X.; Li, H.; Sleen, G.; Basti, M. *Metallothionein III. Dynamic aspects of Metallothionein structure*; Suzuki, K. T., Imura, N., Kimura, M., Eds.; Verlag Basel: Birkhäuser, Switzerland, 1993; pp 57−74.
(20) Savas, M. M.; Petering, D. H.; Shaw, C. F., III. *Inorg. Chem.* **1991**, *30*, 581−583.
(21) Gan, T.; Muñoz, A.; Shaw, C. F., III; Petering, D. H. *J. Biol. Chem.* **1995**, *270*, 5339−5345.
(22) Yu, X.; Wu, Z.; Fenselau, C. *Biochemistry* **1995**, *34*, 3377−3385.
(23) Brouwer, M.; Winge, D. R.; Gray, W. R. *J. Inorg. Biochem.* **1989**, *35*, 289−303.
(24) Zhu, Z.; DeRose, E. F.; Mullen, G. P.; Petering, D. H.; Shaw, C. F., III. *Biochemistry* **1994**, *33*, 8858−8865.
(25) Narula, S. S.; Brouwer, M.; Hua, Y.; Armitage, I. M. *Biochemistry* **1995**, *34*, 620−631.
(26) Zhu, Z.; Goodrich, M.; Isab, A. A.; Shaw, C. F., III. *Inorg. Chem.* **1992**, *31*, 1662−1667.
(27) Li, T.-Y.; Minkel, D. T.; Shaw, C. F., III; Petering, D. H. *Biochem. J.* **1981**, *193*, 441−446.
(28) Faller, P.; Vašák, M. *Biochemistry* **1997**, *36*, 13341−13348.
(29) Sewell, A. K.; Jensen, L. T.; Erickson, J. C.; Palmiter, R. D.; Winge, D. R. *Biochemistry* **1995**, *34*, 4740−4747.
(30) Kull, F. J.; Reed, M. F.; Elgren, T. E.; Ciardelli, T. L.; Wilcox, D. E. *J. Am. Chem. Soc.* **1990**, *112*, 2291−2298.
(31) Fields, G. B.; Tian, Z.; Barandy, G. *Synthetic Peptides: A User's Guide*; Grant, G. A., Ed.; W. H. Freeman and Co.: New York, 1992; p 77.
(32) McCurdy, S. *Pept. Res.* **1989**, *2*, 147−152.
(33) Moore, S.; Stein, W. H. *J. Biol. Chem.* **1954**, *211*, 907−913.

Table 1. Amino Acid Composition and Sequences for the Synthesized β Domains[a]

	polypeptide sequences																												
	1	2	3	4	5	6	7	8	9	10	11	12	13	14	15	16	17	18	19	20	21	22	23	24	25	26	27	28	29	30
β_C	P_{29}	C_{30}	E_{31}	K_{32}	C_{33}	T_{34}	S_{35}	G_{36}	C_{37}	K_{38}	C_{39}	P_{40}	S_{41}	K_{42}	D_{43}	E_{44}	C_{45}	A_{46}	K_{47}	T_{48}	C_{49}	S_{50}	K_{51}	P_{52}	C_{53}	S_{54}	C_{55}	C_{56}	P_{57}	T_{58}
$\beta_{C\rightarrow N}$	P	K	E	C	C	T	S	G	C	K	C	P	S	K	D	C	E	A	K	C	T	C	K	P	C	S	C	S	P	T
β_N	P_1	G_2	P_3	C_4	C_5	K_6	D_7	K_8	C_9	E_{10}	C_{11}	A_{12}	E_{13}	G_{14}	G_{15}	C_{16}	K_{17}	T_{18}	G_{19}	C_{20}	K_{21}	C_{22}	T_{23}	S_{24}	C_{25}	R_{26}	C_{27}	A_{28}			

[a] Subscript numbers indicate the residue position in the amino acid sequence of the lobster holo protein (Cd_6MT).

MeOH/H_2O and 1% acetic acid (as a source of protons) were analyzed and identified using ES-MS in a VG AutoSpec, Fison Instrument, equipped with a Harward syringe driver.

Cd Reconstitution. The apo-β sequences were incubated with a slight excess of Cd^{2+} in Tris-HCl buffer at a pH of ~7.5 and in the presence of 2-mercaptoethanol to avoid oxidation of the thiolates. After concentration, the reaction mixture was loaded onto a Sephadex G-10 desalting column. Cadmium analysis by AAS was used as the detection method to locate the Cd peptide in the eluted fractions. Then, they were treated with Chelex-100, previously activated with 0.1 N HCl and 0.1 N NaOH, to remove adventitiously bound Cd^{2+}. The Cd-β derivatives were characterized by UV−vis, CD, and ES-MS spectroscopies and Cd/SH content. The thiolate content was assayed spectrophotometrically by thiol titration with ′DTNB at 412 nm (ϵ = 13 600 M^{-1} cm^{-1}). [27,34] Cadmium concentrations were quantitated on an Instrumentation Laboratory aa/ae 357 AAS.

Chromatographic Analysis of Dimer Formation. The formation of dimers for the $Cd_3\beta$ derivatives was investigated by analyzing its elution volume from a Sephadex G-25 gel filtration column (1 × 111 cm) previously calibrated with blue dextran (2 000 000 g/mol), cytochrome *c* (12 327 Da), insulin (5 733 Da), and vitamin B_{12} (1 355 Da).

pH Titrations. Spectrophotometric titrations of 13.9 μM Cd-β domains with microquantities of 1 N HCl were carried out in 5 mM Tris-HCl/0.1 M KCl (pH 7.5) until the pH was ~1.8. Then the pH was increased back to 7.4, using 1 N NaOH, in three sequential steps to study the reversibility of the Cd−thiolate binding.

Circular Dichroism (CD) Spectroscopy. Characterization of the apo-β domains and their Cd-β derivatives (20−30 μM) in 5 mM Tris-HCl/0.1 M KCl (pH 2 and 7.5, respectively) was carried out in a Jasco single-beam CD spectropolarimeter model J-715. The absorption corresponding to a blank containing the buffer solution was subtracted from each sample spectrum.

Nuclear Magnetic Resonance (NMR) Spectroscopy. One-dimensional $^{113}Cd\{^1H\}$ NMR spectra of the $^{113}Cd_3\beta$ domains in 5 mM Tris-d_{11}-HCl at pH 7.4 (90% H_2O/10% D_2O) were obtained at 25 °C with a Bruker DPX 300 MHz NMR spectrometer equipped with a 5 mm Z-gradient broad-band probe. Proton decoupling was accomplished using WALTZ composite pulse decoupling during acquisition. The sweep width was 10 638 Hz, centered at 640 ppm. The ^{113}Cd chemical shifts are reported with respect to external 0.1 M $^{113}Cd(ClO_4)_2$ at 0.0 ppm.

One-dimensional ^1H NMR spectra of $^{113}Cd_3\beta$ domains were obtained at 25 EC in a Bruker DPX 300 MHz NMR spectrometer by using WATERGATE for solvent suppression.[35,36] The sweep width was 3591.9 Hz (128 scans were collected).

Reactivity toward DTNB′. To characterize Cd-β derivatives, the reaction with DTNB in 5 mM Tris-HCl/0.1 M KCl at pH 7.5 was spectrophotometrically followed at 412 nm (ϵ = 13 600 M^{-1} cm^{-1}).[27,34] A Perkin-Elmer Lambda 6 UV−vis spectrometer and, when the reaction was too fast for conventional UV spectrophotometers, a stopped-flow spectrometer (Durrum; extensively modified as described elsewhere)[37] were used to study the kinetics of the reaction between $Cd_3\beta_C$, $Cd_5(\beta_{C\rightarrow N})_2$, $Cd_3\beta_{C\rightarrow N}$, and $Cd_3\beta_N$ domains and increasing concentrations of DTNB (varying from 0.3 to 5 mM).

Molecular Modeling Calculations. Molecular mechanic calculations were performed on a Silicon Graphics workstation running Sybyl 6.3, using the MAXIMIN2[38] function that employs the following energy equation:

$$E_{total} = E_{stretch} + E_{bend} + E_{out-of-plane\ bend} + E_{torsion} + E_{vanderWaals} + E_{elect}$$

(34) Jocelyn, P. C. *Methods in Enzymology 143*; Jakoby, W. B., Griffith, O. W., Eds.; Academic Press: London, 1991; pp 44−67.
(35) Piotto, M.; Saudek, V.; Sklenar, V. *J. Biomol. NMR* **1992**, *2*, 661−666.
(36) Sklenar, V.; Piotto, M.; Leppik, R.; Saudek, V. *J. Magn. Reson., Ser. A* **1993**, *102*, 241−245.
(37) Ejnik, J. Ph.D. Thesis, University of Wisconsin−Milwaukee, Milwaukee, WI, 1996.

Table 2. Stoichiometry and Properties of the Synthetic β Domains[a]

after size-exclusion chromatography	after Chelex treatment	MW (kDa)	UV λ_{Cd-S} (nm)	CD λ_{Cd-S} (nm)	δ (^{113}Cd) (ppm)
$Cd_3\beta_C$	$Cd_3\beta_C$	3.4	204, 230, 247	258	664.4, 642.7, 616.2
$Cd_3\beta_{C\rightarrow N}$			210, 221, 247.7	248.3	~650 ($\Delta\upsilon_{1/2}$ = 4330 Hz)
	$Cd_5(\beta_{C\rightarrow N})_2$	6.8	213, 228, 254.2	247.4	~640 ($\Delta\upsilon_{1/2}$ = 4330 Hz)
$Cd_3\beta_N$	$Cd_3\beta_N$	3.4	201, 221, 247	261.8	649.7, 646.7, 641.6[b]

[a] Cadmium content was analyzed by AAS. Protein concentration was analyzed by measuring the SH content. [b] The resonances (δ_{Cd}) for the *N*-acetylated $^{113}Cd_3\beta_N$ cluster stabilized after a period of 6 months. The initial resonances appeared at 659.2, 650.1, and 646.6 ppm. The source of this unique chemistry is under investigation. When the sample was reconstituted a second time after treatment with HCl for 30 min, the initial set of resonances was again observed, indicating that the process is reversible and ruling out the possibility of protein denaturation (i.e., cleavage at the arginine position or the oxidation of the cysteine thiolates).

All of the structures modeled were based on the calculated NMR structures for the synthetic lobster $Cd_3\beta_C$ and $Cd_3\beta_N$ domains of lobster MT (Muñoz et al., unpublished results) which show the same metal−cysteine connectivities and overall folding of the polypeptide chain around the metal ions as those of crab MT.[25] Cadmium−cysteine distances and bond angles were defined according to the experimental NMR values ($d_{Cd-S} \sim 2.52$ Å and $\angle_{S-Cd-S} \sim 109.5°$, which are in good agreement with the values reported for model metal complexes[39] and the published structure of crab MT)[25] to which force constants of 200 kcal/mol·Å^2 for the bond stretching and 20 kcal/mol·rad^2 for the bond angles were applied. Because the tertiary structure of the modified domain is unknown, the modified $\beta_{C\rightarrow N}$ domain was modeled using the cadmium−cysteine connectivities of both the β_C domain and the β_N domain. Dynamic runs followed by minimization were carried out in each case after removing the steric violations by using an algorithm that scanned distances, angles, and torsional angles until the energetically most favorable structure was found. Specific changes in the amino acids adjacent to the cysteine residues of the β_N domain to those of the $\beta_{C\rightarrow N}$ domain were made to study the influence of the electrostatic effects of the side chain on cluster stability.

The distribution of the charges was calculated using the method of Gasteiger-Hückel, and the cutoff value for the nonbonded interactions was set to 8 Å. The minimizations were carried out using the Tripos force-field[40] conjugate-gradient method that incorporates energy changes and displacements[41] and employs a dielectric constant of 1 for the evaluation of electrostatic energies. All of the structures were refined until the final energy change was less than 0.0001 kcal/mol. Molecular dynamic simulations were run in the absence of solvent at 350 K, for a total time of 50 000 fs, using time steps of 1 fs, with velocities assigned by a Gaussian approximation to the Maxwell−Boltzmann distribution. The pairlist was updated every 25 fs. The 20 lowest potential-energy structures obtained at temperature values higher than 320 K were minimized according to the previous protocol until the energy changes observed were less than 0.0001 kcal/mol, and their values were compared.

In a similar fashion, the energies corresponding to the β domains of the human and rabbit MT, as determined by NMR studies,[14,42] were calculated after the minimization step. Because the tertiary structure of the β domain of MT-3 or the growth inhibitor factor, GIF-β, is unknown, it was modeled using the cadmium−cysteine connectivities of the mammalian β domains. Specific changes in the amino acids adjacent to the cysteine residues of the human β domain to those of the MT-3-β domain were carried out to study the impact on cluster stability.

(38) Labanowski, J.; Motoc, I.; Naylor, C. B.; Mayer, D.; Dammkoehler, R. *Quant. Struct.−Act. Relat.* **1986**, *5*, 138−152.
(39) (a) Dance, I.; Fisher, K.; Lee, G. *Metallothioneins: Synthesis, Structure and Properties of Metallothioneins, Phytochelatins and Metal−Thiolate Complexes*; Stillman, M. J., Shaw, C. F., III, Suzuki, K. T., Eds.; VCH: New York, 1991; pp 284−345. (b) Watson, A. D.; Pulla Rao, C. H.; Dorfman, J. R.; Holm, R. H. *Inorg. Chem.* **1985**, *24*, 2820−2826. (c) Lacelle, S.; Stevens, W. C.; Kurtz, D. M., Jr.; Richardson, J. W., Jr.; Jacobson, R. A. *Inorg. Chem.* **1984**, *23*, 930−935.
(40) Clark, M.; Cramer, R.; Van Opdenbosch, N. *J. Comput. Chem.* **1989**, *1*, 982−1012.
(41) Kini, R. M.; Evans, H. J. *J. Biomol. Struct. Dyn.* **1991**, *9*, 475−487.
(42) Messerle, B. A.; Schaffer, A.; Vašák, M.; Kägi, J. H. R.; Wüthrich, K. *J. Mol. Biol.* **1990**, *214*, 765−779.

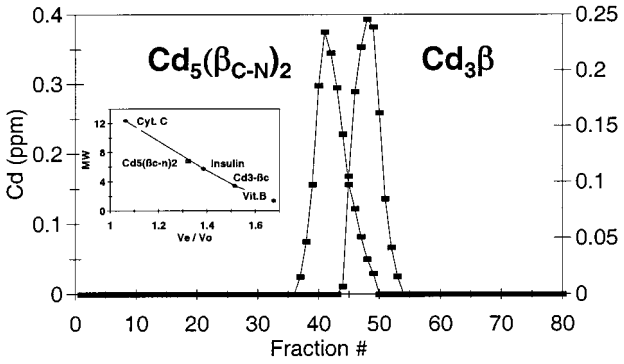

Figure 1. Elution profile for the gel-filtration chromatographic separation of $Cd_3\beta_C$ and $Cd_5(\beta_{C\rightarrow N})_2$ carried out over a Sephadex G-25 column (111 × 1 cm) preequilibrated with 5 mM Tris-HCl (pH 7.5). Insert: calibration curve.

Results

Synthesis. The native β_C and β_N and the modified $\beta_{C\rightarrow N}$ domains of lobster MT-1 were synthesized by solid-phase methods using Fmoc-protected amino acids. After cleavage of the protecting groups, the synthesized domains were purified by reverse-phase HPLC. Sequential treatment with $Hg(CH_3COO)_2$ and 2-mercaptoethanol removed the Acm groups of the cysteine residues and resulted in the corresponding apo-β domains. The UV spectra and Hg analysis indicated that the mercury was removed from each of the polypeptide sequences. Chromatographic separation from the excess of 2-mercaptoethanol was accomplished under acidic conditions to prevent cysteine oxidation. ES-MS carried out at each stage of the deblocking process of these synthetic sequences showed a good agreement with the theoretical values (Figures S1 and S2). Amino acid analysis of the resulting apo peptides confirmed the expected composition.

The reaction of the apo-β domains with $CdCl_2$ under reducing conditions generated $Cd_3\beta$ derivatives which were stable during gel-exclusion chromatography. Analysis of metal and thiolate content carried out by AAS and the DTNB reaction, respectively, confirmed that metal−thiolate clusters with SH/Cd^{2+} ratios equal to 3 are formed in each case. However, treatment with Chelex-100 to remove loosely bound Cd^{2+} revealed a marked difference between native and modified sequences (Table 2). Chromatographic analysis of the Chelex-treated complexes showed that $Cd_3\beta_C$ and $Cd_3\beta_N$ eluted, as expected, at 3.4 kDa, while a species analyzed as $Cd_{2.6}\beta_{C\rightarrow N}$ eluted at 6.8 kDa (Figure 1). This indicates that in the presence of Chelex the modified sequence, $Cd_3\beta_{C\rightarrow N}$, aggregates to a dimer, $Cd_5(\beta_{C\rightarrow N})_2$, with loss of one Cd^{2+} per dimer (eq 1), whereas the native sequences retain their Cd^{2+} content and remain as monomers.

$$2Cd_3\beta_{C\rightarrow N} \rightleftharpoons Cd_5(\beta_{C\rightarrow N})_2 + Cd^{2+} \quad (1)$$

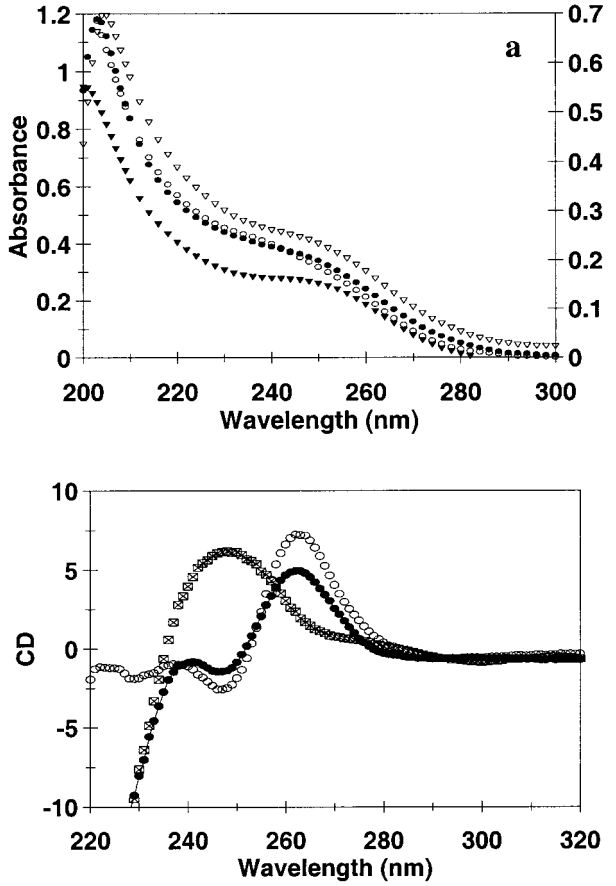

Figure 2. (a) UV−vis spectra for 12 μM Cd-β domains: $Cd_3\beta_C$ (●), $Cd_3\beta_N$ (○), $Cd_5(\beta_{C\rightarrow N})_2$ (▼), and $Cd_3\beta_{C\rightarrow N}$ (▽). (b) CD spectra for 20−30 μM Cd-β_N (○) and $Cd_3\beta_{C\rightarrow N}$ (□) domains and Cd_6MT (●). Spectral measurements were carried out in 5 mM Tris-HCl/0.1 M KCl at pH 7.5, in a PE Lambda 6 UV−vis spectrophotometer and a Jasco CD spectropolarimeter model J-715 (using 2.0 nm band width and 20 mdeg sensitivity, respectively).

UV spectra of the $Cd_3\beta_C$ and $Cd_3\beta_N$ native domains and $Cd_3\beta_{C\rightarrow N}$ and $Cd_5(\beta_{C\rightarrow N})_2$ modified sequences show the absorption band at ∼250 nm, characteristic of ligand-to-metal charge transfer (LMCT; S−Cd; Figure 2). Vašák et al.[16] reported that an increase in the number of bridging thiolates shifts the λ_{max} values of the Cd−S charge-transfer bands toward shorter wavelengths (higher energies). Table 2 lists the λ_{max} obtained for the Cd-β type-B clusters when their absorption bands were mathematically resolved into their three different components. The higher λ_{max} values obtained for Cd $_5(\beta_{C\rightarrow N})_2$ suggest that the dimer contains a smaller fraction of bridging thiolates than the $Cd_3\beta$ monomer, consistent with the loss of one Cd^{2+} per dimer.

The strongest CD signal generated by the $Cd_3\beta_C$ and $Cd_3\beta_N$ domains displayed a maximum at ∼260 nm when the cluster formed and S−Cd−S−Cd−S units were created. This signal, designated as type 2,[16−18,43] is due to symmetry-related interactions between coupled asymmetric cadmium sites (CdS_4). The CD spectrum of the $Cd_3\beta_C$ showed a negative absorption band centered at ∼230 nm (spectrum not shown). It was also observed in the spectrum of the holo protein and is thought to originate from an excitonic coupling between transition dipole moments of bridging thiolate ligands within the $Cd_3\beta_C$ cluster.[44] However,

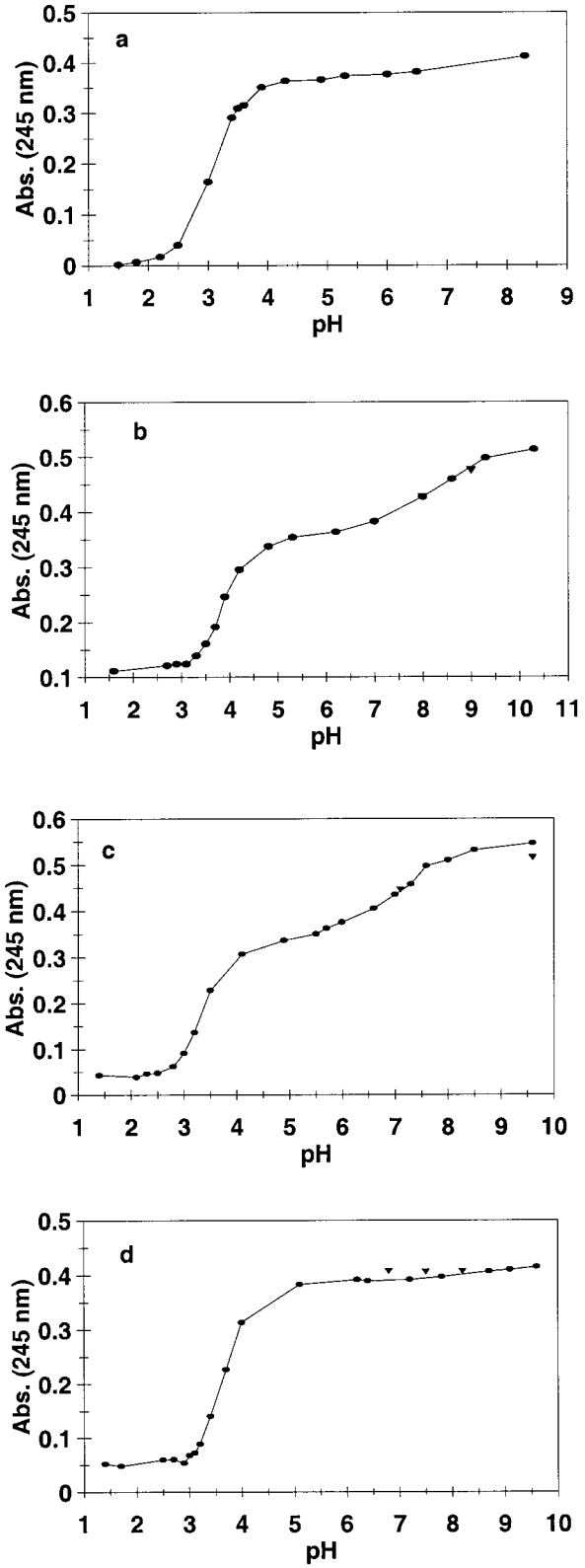

Figure 3. Absorbance at 245 nm vs pH plots for the pH titrations carried out in 5 mM Tris-HCl/0.1 M KCl of 10 μM (a) $Cd_3\beta_C$, (b) $Cd_3\beta_{C\rightarrow N}$, (c) $Cd_5(\beta_{C\rightarrow N})_2$, and (d) $Cd_3\beta_N$ (●, addition of acid; ▼, addition of base).

the CD spectra of $Cd_3\beta_{C\rightarrow N}$ before Chelex treatment and that of $Cd_5(\beta_{C\rightarrow N})_2$ afterward were dominated only by the signals due to the asymmetry of the metal−thiolate binding sites (CdS_4) with a λ_{max} at ∼250 nm (Figure 2 and Table 2). Dissociation of Cd^{2+} ions from the peptides by competition with protons when

(43) Li, Y.-J.; Weser, U. *Inorg. Chem.* **1992**, *31*, 5526−5533.
(44) Law, A. Y. C.; Cherian, M. G.; Stillman, M. J. *Biochim. Biophys. Acta* **1984**, *784*, 53−61.

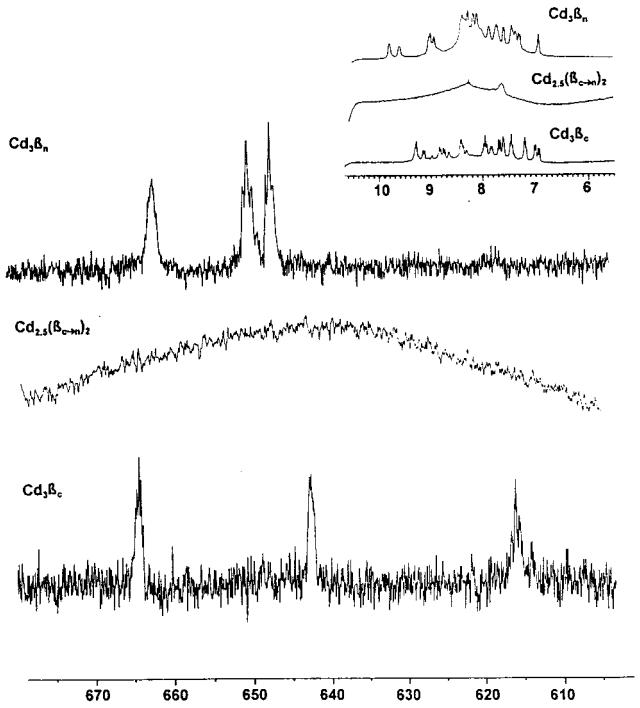

Figure 4. One-dinemsional ^{113}Cd NMR of 3.5 mM $^{113}Cd_3\beta_C$, 5.6 mM $^{113}Cd_3\beta_N$, and 4.5 mM $^{113}Cd_5(\beta_{C\rightarrow N})_2$ in 5 mM Tris-d_{11}-HCl (10% D_2O) at pH 7.5 measured at 66.608 MHz vs $^{113}Cd(ClO_4)_2$. Insert: amide region of the one-dimensional ^{1}H NMR spectra at 300 MHz using WATERGATE solvent suppression.[35,36] The sweep width was 3591.9 Hz (128 scans were collected).

the pH was decreased to 2 resulted in the loss of the CD signals for all four structures.

Both the UV and the CD spectral features of $Cd_3\beta_C$ and $Cd_3\beta_N$ indicated the formation of Cd−thiolate clusters similar to those observed in the holo protein (lobster Cd_6MT). The differences in the λ_{max} values observed in the UV and the CD spectra between the Cd derivatives of the native and modified sequences (Figure 2) signaled differences in their cluster structures.

pH-titration studies were carried out to study the stability of the type-B clusters in these domains. The displacement of Cd^{2+} from each cluster upon increasing the concentration of protons in the media was followed by the changes in the Cd−S charge-transfer absorption band at 245 nm (Figure 3). The behavior observed for the $Cd_3\beta_C$ and $Cd_3\beta_N$ domains was comparable to that observed for the holo protein. The Cd−thiolate linkages started to disappear at pH < 4, as shown by the loss of the absorbance at 245 nm (Figure 3). Titration of the acidified solutions with NaOH resulted in the reconstitution of the Cd clusters. Therefore, the cadmium binding−dissociation process, as in the case of lobster Cd_6MT and mammalian Cd_7MT, was reversible and pH dependent.

$$Cd_3\beta + nH^+ \rightleftarrows 3Cd^{2+} + H_n\beta \qquad (2)$$

However, the pH titration of $Cd_3\beta_{C\rightarrow N}$ and $Cd_5(\beta_{C\rightarrow N})_2$ took place in two distinct stages, where one involves the displacement of Cd^{2+} by the protonation of the Cd−S cluster as the pH decreases from 7 to 2. The half titration pH, ∼3.6, was similar to that for the native domains. The second one is due to the deprotonation of ∼2 and ∼3.5 free cysteines ($\epsilon_{236} = 4.3 \times 10^3$ M^{-1} cm^{-1}) for $Cd_3\beta_{C\rightarrow N}$ and $Cd_5(\beta_{C\rightarrow N})_2$, respectively, as the pH values increased from 7.5 to 9.5. Also, the experimental differences observed in pK_{SH} values (∼8.2 vs ∼7.3 for $Cd_3\beta_{C\rightarrow N}$ and $Cd_5(\beta_{C\rightarrow N})_2$, respectively) suggest changes in the environment of the free cysteines that occurred upon dimer formation.

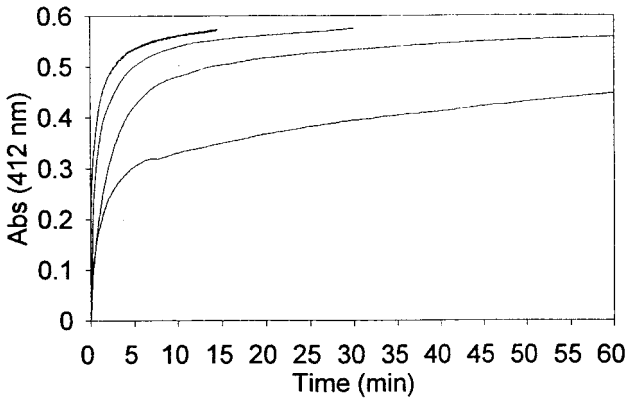

Figure 5. Typical plot for the reaction between 5 μM (a) $Cd_3\beta_C$, (b) $Cd_3\beta_N$, (c) $Cd_3\beta_{C\rightarrow N}$, or (d) $Cd_5(\beta_{C\rightarrow N})_2$ and 0.5 mM DTNB in 5 mM Tris/0.1 M KCl at pH 7.5 followed at 412 nm absorbance corresponding to the TNB formed during the reaction.

The one-dimensional ^{113}Cd NMR chemical shifts of the $^{113}Cd_3\beta_C$ and $^{113}Cd_3\beta_N$ domains given in Table 2 indicate that Cd^{2+} is coordinated to four cysteines, with some of those cysteines bridging between two Cd^{2+} ions (Figure 4). The three resonances (δ_{Cd}) exhibited by the synthetic native lobster domains, $^{113}Cd_3\beta_C$ and $^{113}Cd_3\beta_N$, are consistent with type-B Cd_3S_9 clusters as found in the β_C and β_N domains of the lobster Cd_6MT.[24,26] Thus, ^{113}Cd NMR and ^{1}H NMR, which shows good dispersion at the amide region (Figure 4, insert), confirm that the synthetic native domains have formed stable clusters similar to those found for the natural holo protein.

However, the NMR spectra revealed significant differences between the modified domain structures, $^{113}Cd_3\beta_{C\rightarrow N}$ and $^{113}Cd_5(\beta_{C\rightarrow N})_2$, and the native domains of the holo protein. Both $^{113}Cd_3\beta_{C\rightarrow N}$ and $^{113}Cd_5(\beta_{C\rightarrow N})_2$ exhibited very broad signals in their ^{113}Cd NMR spectrum as well as in the amide region of their ^{1}H NMR spectra (Figures 4 and S3). Similar broadening also occurred in the high-field region of the ^{1}H NMR spectra. These features are consistent with a short T_2 relaxation of the proton resonances, arising from the conformational flexibility of these structures. These NMR characteristics suggest rapid exchange of Cd^{2+} ions between different metal sites and/or multiple solution conformations of the modified domain and dimer (Table 2).

Thiolate Reactivity toward DTNB. The reactivity of the Cd-β species was analyzed by studying the reaction with DTNB. The reaction takes place according to the following scheme, where apo-β_{ox} represents the oxidized metal-free peptide which contains internal disulfide bonds:

$$^9/_2\text{DTNB} + Cd_3\beta \rightarrow \text{apo-}\beta_{ox} + 9\text{TNB} + 3Cd^{2+} \qquad (3)$$

The observed reactions were biphasic for each of the species studied (Figure 5). The $Cd_3\beta$ derivatives showed rate constants with the same order of magnitude as those observed for the holo protein.[26,45] The plots of k_{obs} vs [DTNB] indicated that each phase has DTNB-dependent and -independent components (Table 3). Thus, the overall rate expression for the reaction of

(45) Zhu, Z.; Petering, D. H.; Shaw, C. F., III. *Inorg. Chem.* **1995**, *34*, 4477−4483.
(46) Wilson, J. M.; Wu, D.; Motiu-DeGrood, R.; Hupe, D. J. *J. Am. Chem. Soc.* **1980**, *102*, 359−363.
(47) Whitesides, G. M.; Lilburn, J. E.; Szajewski, R. P. *J. Org. Chem.* **1977**, *42*, 332−338.

Table 3. Rate Constants Calculated for the Reaction between DTNB and Cd-β Species

	k_{uf} (s^{-1})	$k_{1f} \times 10^3$ (s^{-1})	k_{2f} (M^{-1} s^{-1})	$k_{1s} \times 10^3$ (s^{-1})	k_{2s} (M^{-1} s^{-1})
lobs Cd_6MT-1[a]		4.77	5.80	1.01	0.70
lobs Cd_6MT-2[a]		2.27	8.13	1.23	0.66
lobs Cd_5CuMT-2[a]		3.23	2.92	1.34	0.71
$Cd_3\beta_C$ MT-1		5.45	19.1	0.96	0.68
$Cd_3\beta_N$ MT-1		2.98	5.75	0.13	0.36
$Cd_3\beta_{C\rightarrow N}$ MT-1		6.39	28.11	0.37	2.51
$Cd_5(\beta_{C\rightarrow N})_2$ MT-1	0.117			3.10	1.47
Cd peptide$_{49-61}$[b]	0.15	2.59	0.88		

[a] Reference 26. [b] Reference 49. MT peptide$_{49-61}$ corresponds to the amino acid sequence involved in the binding of Cd^{I} (as denominated by ^{113}Cd NMR) of the mammalian $Cd_4\beta$ domain. Whereas the kinetics of $Cd_4\beta$ with DTNB are monophasic, the kinetics of Cd peptide$_{49-61}$ are biphasic.

the $Cd_3\beta$ derivatives, as in the case of the holo protein (Cd_6-MT), was found to be

$$\text{rate} = (k_{1f} + k_{2f}[\text{DTNB}] + k_{1s} + k_{2s}[\text{DTNB}])[Cd_3\beta] \quad (4)$$

The number of thiolates reacting in each step, however, varied with the β domain. While the $Cd_3\beta_C$ has three thiolates which reacted in the fast step and six thiolates in the slow, the $Cd_3\beta_N$ and $Cd_3\beta_{C\rightarrow N}$ domains displayed six and three sulfhydryl groups in these two steps, respectively. If we combine the results for $Cd_3\beta_C$ and $Cd_3\beta_N$, we obtain a total of nine thiolates reacting in each step of the reaction, the same as found for the holo protein Cd_6MT.[26,45]

The second-order components of the rate for $Cd_3\beta_{C\rightarrow N}$ were larger than those observed for the native domains or the holo protein, indicating a more favorable bimolecular reaction between DTNB and the thiolates groups in this modified sequence (Table 3). Furthermore, kinetic monitoring of the reaction for $Cd_5(\beta_{C\rightarrow N})_2$ required stopped-flow methods to resolve a step too fast for conventional spectroscopic measurements. Analysis of the absorbance changes indicated that this reaction was also biphasic, with 6 and 12 thiolates reacting in the ultrafast (uf) and slow steps, respectively. When the k_{obs} values were plotted vs [DTNB] and analyzed, the rate law obtained was

$$\text{rate} = (k_{uf} + k_{1s} + k_{2s}[\text{DTNB}])[Cd_5(\beta_{C\rightarrow N})_2] \quad (5)$$

Free thiol or thiolate groups of proteins always react in a bimolecular process with organic disulfides, such as DTNB or GSSG.[37,46−48] The ultrafast step observed for the reaction between DTNB and $Cd_5(\beta_{C\rightarrow N})_2$ is DTNB concentration independent, although the pH-titration studies suggested the presence of protonated thiols in the dimer. This unusual kinetic behavior of $Cd_5(\beta_{C\rightarrow N})_2$, however, has a precedent in the reaction of the Cd peptide$_{49-61}$ of rabbit liver MT-2 with DTNB,[49] in which analogous DTNB-dependent and -independent kinetic steps are observed. The pervasive differences in the structures and reactivity for $Cd_3\beta_{C\rightarrow N}$ or $Cd_5(\beta_{C\rightarrow N})_2$ in comparison with those of $Cd_3\beta_C$ and $Cd_3\beta_N$ clearly establish that the modified sequence generates new structural interactions with Cd^{2+}, which preserve the reduced thiols in the monomeric and dimeric forms, thus ruling out disulfide formation as the mechanism of dimerization.

(48) Keire, D. A.; Robert, J. M.; Rabenstein, D. L. *J. Org. Chem.* **1992**, *57*, 123−127.
(49) Muñoz, A.; Laib, F.; Petering, D. H.; Shaw, C. F., III. *JBIC, J. Biol. Inorg. Chem.* **1999**, *4*, 495−507.

Table 4. Energy Values after Molecular Mechanic Minimization for $Cd_3\beta_N$, $Cd_3\beta_{C\rightarrow N}$,[a] and Several Mutants of $Cd_3\beta_N$[b]

	local changes in charge	overall charge mutated β_N	energy (kcal/mol)
$Cd_3\beta_N$		0	−179
$Cd_3\beta_N$ ($GPC_4CKD \rightarrow KECCTS$)	+0 → +0	0	−112
$Cd_3\beta_N$ ($DKC_9ECA \rightarrow SGCKCP$)	−1 → +1	+2	+37
$Cd_3\beta_N$ ($A_{12} \rightarrow P$)	+0 → +0	0	−146
$Cd_3\beta_N$ ($E_{10} \rightarrow K$)	−1 → +1	+2	−69
$Cd_3\beta_N$ ($K_8 \rightarrow G$)	+1 → +0	−1	−124
$Cd_3\beta_N$ ($D_7 \rightarrow S$)	−1 → +0	+1	−88
$Cd_3\beta_N$ ($GGC_{16}KT \rightarrow KDCEA$)[b]	+1 → −1	−2	−176
$Cd_3\beta_N$ ($GC_{20}KCT \rightarrow KCTCK$)	+1 → +2	+1	−133
$Cd_3\beta_N$ ($TSC_{25}R \rightarrow KPCS$)	+1 → +1	0	−136
$Cd_3\beta_{C\rightarrow N}$		0	−130

[a] Cd−Cys coordination was set as in $Cd_3\beta_N$. [b] All amino acid changes represent β_N to $\beta_{C\rightarrow N}$ changes in sequence.

Molecular Modeling Calculations. Because the UV−vis, CD, one-dimensional ^{1}H NMR, and one-dimensional ^{113}Cd NMR spectroscopic characteristics as well as kinetic reactivity toward DTNB of the modified domain indicated the presence of less stable, more reactive structures than those of the native domains, we studied the energy differences between the three $Cd_3\beta$ domains using molecular modeling techniques. The energy values for the β_C, β_N, and $\beta_{C\rightarrow N}$ (with Cd−Cys connectivities as in β_N) domains obtained after the minimization step, that followed the dynamic runs at 350 K, were −219, −180, and −130 kcal/mol, respectively. Their relative magnitude supports the higher stability of the native domains and the likelihood that $Cd_3\beta_{C\rightarrow N}$ adopts a different structure. All of the three *N*-acetylated sequences have an overall charge of −2 in the presence of three Cd^{2+} ions, with five basic and three acidic amino acids in addition to the nine cysteine residues that bind to the Cd^{2+} ions. However, there are variations between the positions of (a) the cysteine residues for the β_C and the $\beta_{C\rightarrow N}$ domains and (b) the charged amino acids of the β_N and the $\beta_{C\rightarrow N}$ domains, which might account for the differences in energy observed.

The $\beta_{C\rightarrow N}$ domain (cysteines spaced as in β_N; Table 1) was also modeled by keeping the same Cd−cysteine connectivities of the β_C domain. However, the changes in position of the four cysteine residues resulted in highly distorted metal centers (with shorter Cd−S and Cd−Cd distances, 2.50 ± 0.09 Å instead of 2.56 ± 0.02 Å for d_{Cd-S} and 3.70 ± 0.16 Å instead of 3.24 ± 0.04 Å for d_{Cd-Cd}) when compared with those of the native β_C domain. These types of distortion were not observed when $\beta_{C\rightarrow N}$ was modeled using the Cd−cysteine coordination of β_N. In both cases, the structures lacked the 3−10 helix (residues 41−47) observed in the native β_C. In addition, there is a change in the orientation of the side-chain carboxylic group of Glu45 that moves from the exterior to the interior of the domain in close proximity to one of the Cd^{2+} ions. Thus, Cd−Cys connectivities are partially driven by the position of the cysteine residues.

The energies were calculated for a series of structures retaining the β_N Cd−thiolate connectivities while changing selected non-cysteine residues to convert small regions to the $\beta_{C\rightarrow N}$ sequence (Table 4). We centered these changes around the cysteine residues including Cys4, Cys5, Cys9−Cys11, Cys16, Cys20−Cys22, Cys25, and Cys27. Changes in the regions around Cys4, Cys5, Cys20−Cys22, Cys25, and Cys27 resulted in minor energy variations. The largest increase in energy involved the amino acids adjacent to Cys9 and Cys11. Thus, changes in single amino acids were made in this particular

Table 5. Minimized Energy Values for Human, Rabbit, and GIF $Cd_3\beta$ Domains and Related Mutants of Human $Cd_3\beta$[a]

domain	energy (kcal/mol)
rabbit MT-2 $Cd_3\beta$	+39
human MT-2a $Cd_3\beta$[b]	+42
human $Cd_3\beta$ ($S_7 \rightarrow P$)	+144
human $Cd_3\beta$ ($K_{23} \rightarrow E$)	+38
human $Cd_3\beta$ ($A_9 \rightarrow P$)	+50
human $Cd_3\beta$ ($S_{18} \rightarrow D$)	+41
GIF $Cd_3\beta$[c]	+161

[a] Cd−Cys connectivities were set as in human $Cd_3\beta$. All in silico mutations represent amino acid changes between the sequences of human β domain and GIF-β. [b] Human MT-2a: AcMDP−N**C**$_6$S**C**$_8$-ATGDS**C**$_{14}$T**C**$_{16}$ASS**C**$_{20}$K**C**$_{22}$KE**C**$_{25}$K**C**$_{27}$TS**C**$_{30}$KK. [c] MT-3 (GIF): Ac-MDPET**C**$_6$P**C**$_8$PSGGS**C**$_{14}$T**C**$_{16}$ADS**C**$_{20}$K**C**$_{22}$EG**C**$_{25}$K**C**$_{27}$TS**C**$_{30}$KK.

region. The replacement of the acidic amino acids Glu10 (β_N) by Lys10 ($\beta_{C\rightarrow N}$) and Asp7 (β_N) by Ser7 ($\beta_{C\rightarrow N}$) resulted in final energies after minimization of −69 and −88 kcal/mol, respectively. In contrast, changes in the Cys16 region by introducing two negative charges resulted in a decrease in energy of 40 kcal/mol. Thus, local changes in charge may be responsible for the energy increases, although there is not a linear relationship between the energy and the overall charge of the cluster. Similar results were obtained when the structure of crab MT was used as a basis for the calculations.

The spectroscopic characteristics of $Cd_3\beta_{C\rightarrow N}$ and the β domain of Cd_3MT-3 (β-GIF) resemble one another. Both display a shifted UV−CD band and have lost the characteristic three-resonance ^{113}Cd NMR spectrum of the β domain.[28] It was hypothesized that changes in a small number of non-cysteine amino acids in the β domain of MT-3 (GIF) in comparison with MT-1 or MT-2 account for its peculiar spectral properties. Thus, the energy of the $Cd_3\beta$ domain of GIF was calculated using a similar approach.

In this case, the structure was modeled using the Cd−cysteine connectivities of the $Cd_3\beta$ domain of human MT-1 or MT-2, which have sequences homologous to MT-3 (GIF) with the cysteine residues located in the same positions along the polypeptide sequence. The energy values calculated for the β domains of human MT and GIF were +42 and +161 kcal/mol, respectively (Table 5), suggesting a lower stability for the β-GIF domain. When the energies of a series of structures were calculated in which changes in the non-cysteine residues of human β were converted to those of β-GIF (MT-3), it was observed that a single change, the insertion of a proline residue between Cys5 and Cys7, resulted in an increase of energy comparable to the one observed for $Cd_3\beta$-GIF (Table 5). However, replacement of other single amino acids including those that changed the overall charge of the cluster (Lys22Glu and Ser18Asp) resulted in only minor changes in energy (Table 5).

Discussion

Structural NMR studies carried out with crustacean MTs, which consist of two domains containing Cd_3S_9 clusters, have shown that the specific Cd−cysteine coordination differs markedly between the β_C and the β_N domains. The two domains of crustacean MTs and the β domain of mammalian MTs each contain nine cysteine residues that are dispersed somewhat differently within their sequences. As a result, peptide folding around the three clusters also differs.[24−26] Yet, the three sequences bind Cd^{2+} ions to form three-metal cadmium−thiolate clusters that are structurally identical with three bridging and six terminal thiolate ligands.[24,26] Thus, three structurally different and naturally occurring β domains have been identified.[12,14,24] From their existence, it is clear that stable type-B clusters can be formed from at least several sequences exhibiting some differences in location of the cysteine ligands for Cd^{2+}. On the basis of these results, one can consider whether the only requirement for the formation of stable type-B, Cd_3S_9, clusters is the presence of nine cysteine residues dispersed along the peptide sequence or whether other residues in the sequence contribute to their structure, stability, and reactivity.

To study the effects that the position of the cysteine residues and the characteristics of the other amino acid side chains adjacent to the cysteines exert on the Cd−CyS connectivities and the reactivity of the $Cd_3\beta$ clusters, three different sequences based on the β domains of lobster MT (β_C, β_N, and $\beta_{C\rightarrow N}$) were synthesized using the Merrifield solid-phase method. β_C and β_N correspond to the native C-terminal and N-terminal domains of lobster MT-1, respectively. $\beta_{C\rightarrow N}$ retains the amino acid composition of β_C as well as most of its sequence (80% homology in non-cysteine amino acids, 70% overall), but the cysteine residues are placed in the positions corresponding to those of β_N.

ES-MS, amino acid analysis, and chemical characterization demonstrated that the chemical synthesis of the native apo-β_C and apo-β_N domains of lobster MT-1 was successfully accomplished. Stable $Cd_3\beta_C$ and $Cd_3\beta_N$ clusters were generated when the synthetically prepared native lobster domains were reconstituted with cadmium ions. Spectroscopic characterization of these cadmium derivatives demonstrated (1) an absorption band at ∼250 nm due to ligand-to-metal charge transfer, LMCT,[16] (2) a CD-signal centered at ∼260 nm due to interactions between asymmetrically coupled pairs of Cd−S units within the binding site generated when the cluster forms,[16,17,43] and (3) one-dimensional ^{113}Cd NMR chemical shifts between 610 and 670 ppm, reflecting the formation, above pH 4, of Cd−thiolate clusters analogous to those found in lobster MT[24,26] (Table 2 and Figures 2 and 4).

Mammalian Cd_7MTs exhibit biphasic kinetics in their reactions with the aromatic disulfide DTNB[27,50,51] in which each step is due to the reaction of one of the two domains: the $[Cd_4\alpha]^0$ domain is responsible for the fast step[20] and the $[Cd_3\beta]^{2-}$ domain for the slow.[52] These results led to two hypotheses: (1) the differences in reactivity are due to differences in cluster structure, type-A Cd_4S_{11} vs type-B Cd_3S_9, or (2) they are imposed by the protein structure surrounding the domains. The latter could involve either steric features of the folding of the peptide backbone around the cluster or detailed placement of the side-chain groups of specific non-cysteine amino acids. The first hypothesis was ruled out when the reaction between DTNB and lobster Cd_6MT, with two type-B Cd_3S_9 clusters each having a net charge of −1, was studied, and biphasic kinetic behavior was also observed.[26,45] Unlike the monophasic reactions of the mammalian α and β domains, biphasic kinetics with rate constants comparable to those of the holo protein (Cd_6MT) were observed when each of the synthesized native domains, $Cd_3\beta_C$ and $Cd_3\beta_N$, reacted with DTNB (Table 3). Thus, each of the three naturally occurring $Cd_3\beta$ domains (one from mammalian MT and two from lobster MT), containing the same type-B cluster structure but distinct Cd−cysteine connectivities and folding of the peptide around

(50) Backowski, G. Ph.D. Thesis, University of Wisconsin−Milwaukee, Milwaukee, WI, 1984.
(51) Pu, C. Ph.D. Thesis, University of Wisconsin−Milwaukee, Milwaukee, WI, 1991.
(52) Muñoz, A.; Petering, D. H.; Shaw, C. F., III. *Inorg. Chem.* **1999**, *38*, 5655−5659.

the cluster, reacts differently with DTNB. These results suggested that particular features of the folding of the amino acid sequences result in the different kinetic behaviors of the mammalian and crustacean β domains.

Two alternative hypotheses were initially established for the study of the $\beta_{C\rightarrow N}$ domain reconstituted with Cd^{2+}. (1) If only the position of the cysteine residues determines folding of the peptide backbone and reactivity of the peptide around the cluster, the $\beta_{C\rightarrow N}$ and β_N domains would be expected to have the same Cd−CyS connectivities and display similar patterns of chemical reactivity. (2) If the non-cysteine amino acid sequence also serves as a determinant of folding and reactivity, the $\beta_{C\rightarrow N}$ domain might behave like the β_C domain, which has a similar though not identical sequence of non-cysteine residues.

As shown in this study, marked differences distinguish the $\beta_{C\rightarrow N}$ domain from β_C and β_N and thereby contradict both of these hypotheses. The modified $Cd_3\beta_{C\rightarrow N}$ domain lost cadmium to ChelexJ and formed a dimer, $Cd_5(\beta_{C\rightarrow N})_2$, as shown by analytical gel-exclusion chromatography. Both monomer and dimer are formed via Cd−thiolate interactions, but their distinctive spectroscopic features (UV and CD λ_{max} and a very broad one-dimensional ^{113}Cd NMR signal) imply that significant structural differences exist in comparison with the native domains. According to the pH-titration studies, the monomer and dimer of the modified sequence contain two and four partially protonated cysteine residues, respectively. In addition, unlike the native domains, the ^{1}H NMR features for the $Cd_5(\beta_{C\rightarrow N})_2$ and $Cd_3\beta_{C\rightarrow N}$ structures suggest large conformational flexibility. There were also marked differences between synthetic native and modified domains in their reactivity toward DTNB and in response to pH changes. The larger values of the second-order components of the rate law for the reaction between DTNB and $Cd_3\beta_{C\rightarrow N}$, compared to those of the native domains, suggest that easier access of the electrophilic disulfide to the thiolate groups of the modified domain facilitated the bimolecular reaction. The ultrafast reaction of $Cd_5(\beta_{C\rightarrow N})_2$ with DTNB and the second step in the pH titration (pH ~9) might be attributable to the presence of protonated thiols. In turn, they may be responsible for the conformational flexibility, suggested by ^{1}H NMR, that facilitates the Cd^{2+} exchange among binding sites and causes the broad nondescript ^{113}Cd NMR signal. Similar broadening of the ^{1}H NMR spectrum has been reported for the $Cd_3\beta$ MT-3 domain (β-GIF).[28]

The DTNB concentration independence observed for the ultrafast step of the reaction of $Cd_5(\beta_{C\rightarrow N})_2$ was also seen in the ultrafast step of the reaction with the Cd peptide$_{49-61}$ of rabbit liver MT-2.[49] The rate-limiting step in the reaction of the Cd peptide$_{49-61}$ is the breaking of the Cd−thiolate bonds. In the case of $Cd_5(\beta_{C\rightarrow N})_2$, rapid conformational rearrangements of the dimer suggested by the NMR results might account for a rate-limiting process and are under investigation.

To account for the spectroscopic and kinetic features observed, two possible structures are proposed for the $Cd_3\beta_{C\rightarrow N}$ and $Cd_5(\beta_{C\rightarrow N})_2$ clusters (Figure 6). For the monomer, $Cd_3\beta_{C\rightarrow N}$, an equilibrium of several structures is proposed, in which two cysteines and two oxygen donor atoms exchange as members of the ensemble of the Cd ligands. The open cluster including free thiols may result in the observed second process of the pH titration and the large second-order rate constant of its reaction with DTNB. In this model, these structures tend to dimerize with the loss of one Cd^{2+} and the consequent increase in the number of terminal cysteines. The resulting dimer (Figure 6) with a C_2 axis of rotation generates a more open structure with

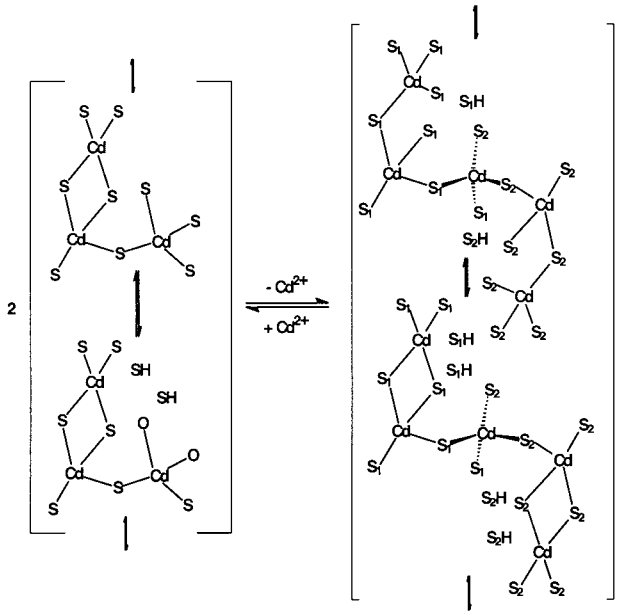

Figure 6. Schematic representations of possible structures for the $Cd_3\beta_{C\rightarrow N}$ and $Cd_5(\beta_{C\rightarrow N})_2$ metal−thiolate clusters. The subscripts 1 and 2 on the sulfur atoms identify the two peptides involved in the formation of the dimer.

additional free thiols, as suggested by its reaction with DTNB and its pH titration.

Molecular modeling calculations suggested that the instability of the $\beta_{C\rightarrow N}$ cluster arises primarily from the replacement of the amino acids adjacent to Cys9 and Cys11, particularly Asp7 and Glu10 (Table S1). Interestingly, Asp7 is conserved in both isoforms of crustacean MT and lobster MT. Replacement of Asp7 (β_N) by Ser ($\beta_{C\rightarrow N}$) resulted in the loss of three hydrogen bonds, involving the side-chain carboxylic group of Asp as the acceptor and the amide−nitrogen of the Lys8 and the amine group hydrogens of Lys6 as the donors. The donor−acceptor distances from Lys8(NH_{amide}) and Lys6(NH_3^+) to Asp7(COO^-) were 1.7 and 1.6 Å, respectively, whereas those to Ser7(OH) of the mutant were 2.5 and 2.8 Å, thus precluding H-bonding interactions (Figure 7). As a result, in the minimized structure of the $Cd_3\beta_N$−Asp7Ser mutant the backbone folding around the metal cluster differed somewhat from that in the minimized structure of native $Cd_3\beta_N$. The substitution of Glu10 by Lys resulted in an increase on the solvent exposure of the cluster. On the basis of two-dimensional NMR experiments (Muñoz and Petering, unpublished results), the side chain of Glu10 is folded toward the interior of the cluster in β_N, covering the thiol group of Cys5, instead of orienting toward the exterior of the domain as in the Glu10Lys mutant (Figure 8).

That a single, non-cysteine amino acid substitution in the MT β domain sequence can dramatically alter the properties of the metal−thiolate cluster is also suggested by molecular modeling results related to $Cd_3\beta$ MT-3 (β-GIF). Although the MT-3 β domain differs in only seven amino acid residues from the MT-1 or MT-2 β domains, they exhibit different Cd cluster properties and structures.[28,53] $Cd_3\beta$ MT-3 has a much higher calculated energy, supporting the view that non-cysteine residues are important in the folding and stability of the clusters. Among the calculated energies of MT-2 β mutants bearing one of each of the amino acid substitutions in MT-3, only that for the Ser7Pro substitution increased to an energy value approaching

(53) Bogumil, R.; Faller, P.; Binz, P.-A.; Vašák, M.; Charnock, J. M.; Garner, C. D. *Eur. J. Biochem.* **1998**, *255*, 172−177.

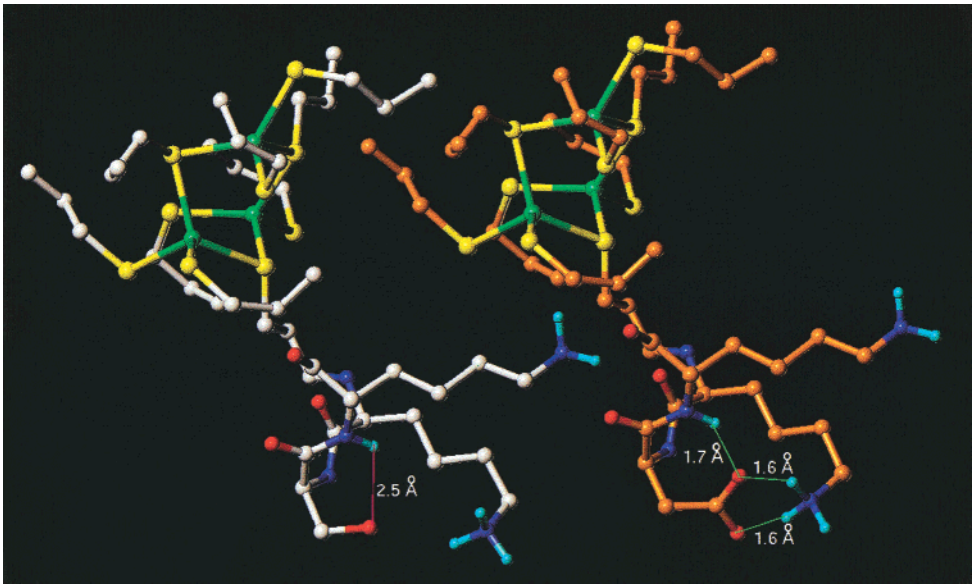

Figure 7. Ball and stick representation of the Cd_3SCy_9 clusters for the native β_N (in orange) and its mutant Asp7Ser (white) showing the distances for the possible H bonds between residues Lys6, Lys8, and Asp7 or Ser7.

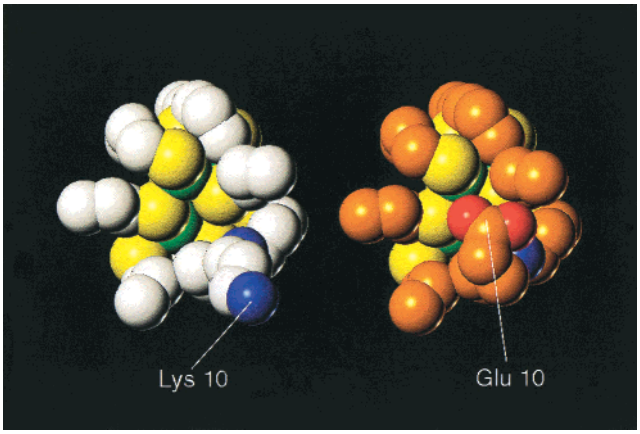

Figure 8. Space-filling representation of the metal−cysteine clusters (Cd_3S_9) of the minimized structures, using the Tripos force field in SYBYL, for $Cd_3\beta_N$ (orange) and the mutant $Cd_3\beta_N$−Glu10Lys (white). The figure shows the differences generated on the solvent exposure of the metal cluster as a result of the changes in the orientation of the side chain of residue 10 (sulfur, yellow; cadmium, green; nitrogen, blue; oxygen, red).

that obtained for β-GIF. The other changes such as Asn5Thr, Ala9Pro, Ser18Pro, or Lys23Glu resulted in only minor variations in energy (Table 5). It appears that it is the insertion of proline at position seven that generates the instability and perhaps greater reactivity of the GIF β domain. The hypothesis that the Cys6−Pro7−Cys8−Pro9 sequence of MT-3 is necessary for its proposed biological function, regulation of Zn^{2+} concentrations at the brain neuronal synapses,[29] is consistent with these findings.

In summary, the results presented here indicate that the modified lobster $\beta_{C\rightarrow N}$ domain does not form the same type of stable clusters as the native β_C or β_N domains. Instead, it displays different spectroscopic features and kinetic reactivity and a tendency to undergo dimerization. Molecular modeling strongly suggests that even a single non-cysteine amino acid can be a critical determinant of MT domain stability. Thus, we have demonstrated that the structure, stability, and reactivity of the type-B Cd_3S_9 clusters depend on the detailed sequence of amino acids in the β domains and not simply the placement of cysteine residues within the sequence. Both the folding of the peptides to create Cd−thiolate clusters and the reactivity of the resultant Cd−thiolate clusters reflect subtle relationships between the sequence of cysteine residues and the nature and placement of neighboring non-cysteine amino acids.

Acknowledgment. This research was supported by U.S. NIH Grants ES 04026, ES 04184, and DK 51308.

Supporting Information Available: Figures S1−S3 and Table S1, displaying information described in the text. This material is available free of charge via the Internet at http://pubs.acs.org.

IC000485S